JIRSS (2025)
Vol. 24, No. 01, pp 139-156
DOI: 10.22034/jirss.2025.2013301.1039

A Double Multivariate Homogeneously Weighted Moving Average Control Chart: An Extension Work

Samson O. Ugwu[1], Akaninyene U. Udom[1], Everestus O. Ossai[1], Uchenna C. Nduka[1],

[1] Department of Statistics, University of Nigeria, Nsukka, Enugu State, Nigeria.

Received: 10/10/2023, Accepted: 12/10/2025, Published online: 07/12/2025

Abstract. This work extends an existing multivariate homogeneously weighted moving average (MHWMA)-control chart to a multivariate double homogeneously weighted moving average (MDHWMA)-control chart aimed at a more efficient monitoring of the process mean vector. Like the MHWMA-control chart, the MDHWMA-control chart statistic assigns a specific weight to the current observation, and the remaining weight is evenly assigned among the previous observations but unlike the MHWMA-control chart, the MDHWMA-control chart statistic utilizes the information contained in the observations twice. We present the design structure of the MDHWMA-control chart and on the basis of the average run length, standard deviation of the average run length and the median run lengths (ARL, SDRL & MRL) compare the performance with the MHWMA-control chart in relations to Hotelling's χ^2-chart, multivariate cumulative sum (MCUSUM)-chart and the multivariate exponentially weighted moving average (MEWMA)-chart. The comparison showed that the proposed (MDHWMA)-control chart has a better performance than the competing charts especially for small shifts. .

Keywords. Control charts, Multivariate control chart, Memory-type control chart, Average run length, Median run length, Standard deviation run length.

MSC: 62-XX, 62Rxx, 62R10.

Corresponding Author: Samson O. Ugwu (offorma.ugwu@unn.edu.ng).
Akaninyene U. Udom (akaninyene.udom@unn.edu.ng).
Everestus O. Ossai (everestus.ossai@unn.edu.ng).
Uchenna C. Nduka (uchenna.nduka@unn.edu.ng).

1 Introduction

No manufacturing process is without variations. These variations can either be of natural or assignable causes (Abbasi et al., 2015). Therefore, to guarantee quality in manufacturing processes amid these variations, Statistical Process Control (SPC) becomes inevitable. Abbasi et al. (2015) stated that SPC is a collection of statistical techniques used to monitor the quality characteristics of manufacturing processes. Adegoke et al. (2019) said that among these techniques, control charts are the most popular and sophisticated tools for tracking a process and identifying whether it is in control (IC). Different types of control charts have been developed in the SPC literature and each is either a memory-less or memory-type control chart. The latter came as a solution to the weakness of the former. Quality control charts are memory-less when they don't refer to the past information of the process, instead, they make due of only the information in the current observation or vector of current observations for the monitoring processes but they are memory-type if otherwise (Testik et al., 2003). The Shewhart chart, Hotelling's Chi-square chart, and of course all the Shewhart-based control charts are memory-less and therefore use only the information from the current observation in their monitoring processes. It has been established in the literature that memory-less type of charts is effective only in identifying large shifts in the process parameters (Saber et al., 2021). To increase the sensitivity of these quality control charts in detecting small-to-moderate shifts in the process parameters, different memory-type charts have been proposed and developed. These charts were found to be more sensitive in detecting small-to-moderate shifts when compared to the memory-less charts, see Page (1954), Roberts (1959), Crosier (1988) and Pignatiello and Runger (1990).

For any control chart, the objective is to have the smallest possible out-of-control (OOC) average run length (ARL_1), which is the average number of the plotted samples needed by the chart to detect an OOC condition while the in-control (IC) average run length (ARL_0) is the average number of plotted samples until an OOC signal is raised by the chart. To attain this objective, several advancements and modifications to the existing charts have been proposed, see Lucas (1982) on the development of Shewhart-CUSUM chart, Lucas and Saccucci (1990) on the study of the Shewhart-EWMA chart to trace shifts in the process location, Lucas and Saccucci (1990) on the study of the steady-state behavior of the EWMA chart for monitoring the mean of the quality characteristic, Shamma and Shamma (1992) on the development of a double EWMA chart, Abbas et al. (2013) on the development of a mixed EWMA-CUSUM chart, Zaman et al. (2014) on the development and investigation of a mixed CUSUM-EWMA chart, Abbas et al. (2020) on the design of a double progressive mean chart for the process mean shift and Aslam et al. (2018) on the investigation of a hybrid EWMA scheme to monitor process variability to mention but a few.

The EWMA chart and all control charts based on the EWMA structure assign larger weights to the most current observation and lesser weights to the less current observations but Hunter (1986) showed that the main drawback of the plotting statistic of the EWMA chart lies in this manner of assignment of weights. As a solution to this, Abbas (2018) designed and studied the homogeneously weighted moving average (HWMA)

charting scheme which assigns a certain weight to the current process observation and the remaining weight is homogeneously assigned to the rest of the observations of the process. Also, see Letshedi et al. (2022) on the application of the homogeneously weighted moving average (HWMA) charting scheme when normality assumption is violated and Luke et al. (2023) on the integration of machine learning on the study of the a new multivariate extended homogeneously weighted moving average monitoring scheme.

In industries of today, there is a fast-growing development in data acquisition. With these computerized tools and an abundance of available data, additional factors or variables affecting individual processes have been uncovered. With more than one factor or variable affecting or determining a process, the univariate or single variable approach used in most of the traditional process charts cannot effectively monitor such processes as these variables create a multivariate setting to determine the outcome of the processes. As a result, multivariate process control (MPC) procedures in which several related process parameters are jointly monitored are one of the most rapidly developing areas in (SPC) (Seif et al., 2011). To address this problem, Hotelling (1947) proposed and applied a multivariate process control tool which is known as the multivariate chi-square control chart. However, the Multivariate chi-square chart is a memory-less type chart and as such isn't effective in detecting small-to-moderate shifts in the process parameters. Reacting to the need of increasing the sensitivity of the MPC procedure, different multivariate memory-type schemes have been proposed in the literature, to this effect, see Crosier (1988) on multivariate generalizations of cumulative sum quality control schemes, Pignatiello and Runger (1990) on comparisons of multivariate CUSUM charts, and Lowry et al. (1992) on a multivariate exponentially weighted moving average control chart. To enhance the performance in detecting small-to-moderate shifts, several extension of EWMA chart have also been proposed in the literature, see Hawkins and Maboudou-Tchao (2007) on Self-Starting Multivariate Exponentially Weighted Moving Average Control Charting, Kramer and Schmid (1997) on EWMA charts for multivariate time series, Park and Jun (2015) on a new multivariate EWMA chart via multiple testing and Yumin (1996) on an improvement for MEWMA in multivariate process control. However, on the grounds of Hunter (1986) on the setback of the the plotting statistic of the EWMA chart and all its extensions, Abbas (2018) designed and studied the homogeneously weighted moving average (HWMA) charting scheme which assigns a certain weight to the current process observation and the remaining weight is homogeneously assigned to the rest of the observations of the process. Abid et al. (2020) extended the work of Abbas (2018) to the double homogeneously weighted moving average control charts (DHWMA) which utilizes the information from the process twice but which assigns weight same way as Abbas (2018). It was reported in the paper that DHWMA control chart outperformed the HWMA control chart in OOC detection. Adegoke et al. (2019) extended the work of HWMA-chart of Abbas (2018) to a multivariate scheme and called it a multivariate homogeneously weighted moving average (MHWMA) control chart for monitoring the multivariate mean vector of the process variables. The MHWMA control chart performance was compared with the Hotelling's χ^2-chart, the multivariate cumulative sum (MCUSUM) control chart, and the multivariate exponentially moving average (MEWMA) control chart. The comparison showed that the (MHWMA) control chart is

superior to the other multivariate counterparts.

To the best of our knowledge, no extension of the work of the Adegoke et al. (2019) exists in the literature, therefore, just like the DHWMA control chart by Abid et al. (2020), this work proposes an extension of the MHWMA control chart to a multivariate double homogeneously weighted moving average (MDHWMA) control chart.

The remainder of this work will be structured as follows. The reviews of the design structures of the univariate HWMA and DHWMA by Abbas (2018) and Abid et al. (2020) will be presented in Section 2 under Subsections 2.1 and 2.2 respectively. In Section 3, we present the design structure of the MHWMA and in Section 4, the design structure of the new chart, MDHWMA will be presented. We present the simulation study in Section 5 while Section 6 is for the numerical application of the MDHWMA control chart and the conclusion of the work is in Section 7.

2 Design Structures of the Univariate HWMA and DHWMA Charts

2.1 Design Structure of HWMA control chart

Suppose that Y_{tj}; t=1, 2, 3, ... and j = 1, 2, 3, ..., n is a quality characteristic of interest taken from a normal distribution with mean and standard deviation μ_Y and σ_Y respectively. Abbas (2018) stated that the charting statistic of the HWMA is given by

$$H_t = w\bar{Y}_t + (1-w)\,\bar{\bar{Y}}_{t-1} \tag{2.1}$$

where $\bar{Y}_t$ is the mean of the observations taken at the time t, $\bar{\bar{Y}}_{t-1}$ is the mean of the previous $t-1$ samples, w is the smoothing/sensitivity parameter which satisfies $0 < w \leq 1$ and the starting value of $\bar{\bar{Y}}_0 = \mu_0$. The mean and variance of the charting statistic H_t are given by; $E(H_t) = \mu_0$ and $Var(H_t) = \frac{\sigma_0^2}{n}\left[w^2 + \frac{(1-w)^2}{t-1}\right]$ respectively. Therefore, the control limits of HWMA chart are

$$\begin{aligned} LCL_t &= \mu_0 - K\sqrt{\frac{\sigma_0^2}{n}w^2} \\ CL &= \mu_0 \\ UCL_t &= \mu_0 + K\sqrt{\frac{\sigma_0^2}{n}w^2},\ for\ t = 1 \end{aligned}$$

$$\begin{aligned} LCL_t &= \mu_0 - K\sqrt{\frac{\sigma_0^2}{n}\left[w^2 + \frac{(1-w)^2}{(t-1)}\right]} \\ CL &= \mu_0 \\ UCL_t &= \mu_0 + K\sqrt{\frac{\sigma_0^2}{n}\left[w^2 + \frac{(1-w)^2}{(t-1)}\right]},\ for\ t > 1 \end{aligned}$$

Note that in the case where $n = 1$, equation (2.1) simplifies to $H_t = wY_t + (1 - w)\,\bar{Y}_{t-1}$. The HWMA chart signals a shift from the IC target if the charting statistic, H_t, exceeds the control limits.The chart was compared with the existing memory-type control charts and found to have a better performance for small to moderate shifts, especially at small values of the smoothing parameter (w).

2.2 Design Structure of DHWMA-chart

By using the same conditions already defined in Subsection 2.1, Abid et al. (2020) extended the HWMA control chart to DHWMA control chart which proved to be more efficient than the former. The DHWMA chart statistic uses the sample information twice and hence named, double homogeneously weighted moving average. Therefore, the DHWMA control chart statistic is:

$$DH_t = wH_t + (1 - w)\,\bar{\bar{Y}}_{t-1} \tag{2.2}$$

By substituting equation (2.1) into equation (2.2) and simplifying, we have;

$$DH_t = w^2\bar{Y}_t + \left(1 - w^2\right)\bar{\bar{Y}}_{t-1}$$

where $\bar{Y}_t$, w and $\bar{\bar{Y}}_{t-1}$ are as already defined in equation (2.1). The mean and variance of this statistic are given by; $E\left(DH_t\right) = \mu_0$ and $Var\left(DH_t\right) = \frac{\sigma_0^2}{n}\left[w^4 + \frac{\left(1-w^2\right)^2}{t-1}\right]$ respectively. The development of the DHWMA control chart was motivated by the presence of the DEWMA control chart in the literature that improved the EWMA. Following the mean and variance of the control statistic, the control limits of the DHWMA control chart are

$$\begin{aligned} LCL_t &= \mu_0 - K\sqrt{\frac{\sigma_0^2}{n}w^4} \\ CL &= \mu_0 \\ UCL_t &= \mu_0 + K\sqrt{\frac{\sigma_0^2}{n}w^4},\ when\ t = 1 \end{aligned} \tag{2.3}$$

$$\begin{aligned} LCL_t &= \mu_0 - K\sqrt{\frac{\sigma_0^2}{n}\left[w^4 + \frac{(1-w^2)^2}{(t-1)}\right]} \\ CL &= \mu_0 \\ UCL_t &= \mu_0 + K\sqrt{\frac{\sigma_0^2}{n}\left[w^4 + \frac{(1-w^2)^2}{(t-1)}\right]},\ when\ t > 1 \end{aligned} \tag{2.4}$$

Note that in the case where $n = 1$, equation (2.2) simplifies to $DH_t = wH_t + (1 - w)\,\bar{Y}_{t-1}$, equations (2.3) and (2.4) and $Var\left(DH_t\right)$ simplify to equations (2.5), (2.6) and (2.7)

respectively

$$\begin{aligned} LCL_t &= \mu_0 - K\sqrt{\sigma_0^2 w^4} \\ CL &= \mu_0 \\ UCL_t &= \mu_0 + K\sqrt{\sigma_0^2 w^4},\ when\ t = 1 \end{aligned} \tag{2.5}$$

$$\begin{aligned} LCL_t &= \mu_0 - K\sqrt{\sigma_0^2\left[w^4 + \frac{(1-w^2)^2}{(t-1)}\right]} \\ CL &= \mu_0 \\ UCL_t &= \mu_0 + K\sqrt{\sigma_0^2\left[w^4 + \frac{(1-w^2)^2}{(t-1)}\right]},\ when\ t > 1 \end{aligned} \tag{2.6}$$

$$Var\left(DH_t\right) = \sigma_0^2\left[w^4 + \frac{\left(1-w^2\right)^2}{t-1}\right] \tag{2.7}$$

3 Design Structure of the MHWMA

Suppose we have $p \times n$ independently and identically distributed multivariate normal random variables; $\boldsymbol{Y_1, Y_2, Y_3, \ldots, Y_p}$ with mean vector $(\boldsymbol{\mu_0})$ and the covariance matrix $\boldsymbol{\Sigma_0}$, Adegoke et al. (2019) extended the univariate HWMA control chart, proposed by Abbas (2018) to a multivariate case denoted as MHWMA control chart and the control chart statistic is

$$\boldsymbol{MH_t} = W\bar{\boldsymbol{Y}}_{\boldsymbol{t}} + (I - W)\,\bar{\bar{\boldsymbol{Y}}}_{\boldsymbol{t-1}} \tag{3.1}$$

where; $\boldsymbol{I}$ is a diagonal matrix of $1's$, $\boldsymbol{W}$ $= p \times p$ diagonal square matrix with the smoothing or sensitivity parameters w_k, $k = 1, 2, \ldots, p$ along the diagonal such that $0 < w_k \leq 1$ and $\bar{\bar{Y}}_0$ is the mean vector at the initial point ($t = 1$) which is the same as the mean vector of the distribution, μ_0. In the occasions where the sensitivity parameter which determines the weight of each observation is equal across the variables, then the charting statistic of MHWMA control chart becomes

$$\boldsymbol{MH_t} = w\bar{\boldsymbol{Y}}_{\boldsymbol{t}} + (1 - w)\,\bar{\bar{\boldsymbol{Y}}}_{\boldsymbol{t-1}} \tag{3.2}$$

The mean and the covariance matrix of the charting statistic of $\boldsymbol{MH_t}$ have been proven and are given as $E\left(\boldsymbol{MH_t}\right) = \boldsymbol{\mu_0}$ and $\Sigma_{\boldsymbol{MH_t}} = \begin{cases} \frac{w^2}{n}\Sigma_0 & t = 1 \\ \frac{w^2}{n}\Sigma_0 + (1-w)^2\,\frac{\Sigma_0}{n(t-1)} & t > 1 \end{cases}$. Note that in the case where $n = 1$, equation (3.2) becomes $\boldsymbol{MH_t} = w\boldsymbol{Y_t} + (1 - w)\,\bar{\boldsymbol{Y}}_{\boldsymbol{t-1}}$ and Σ_{MH_t} becomes $\begin{cases} w^2\Sigma_0 & t = 1 \\ w^2\Sigma_0 + (1-w)^2\,\frac{\Sigma_0}{(t-1)} & t > 1 \end{cases}$. The MHWMA control chart statistic is given as in equation (3.3)

$$T_t^2 = (\boldsymbol{MH_t} - \boldsymbol{\mu_0})' \, \Sigma_{\boldsymbol{MH_t}}^{-1} \, (\boldsymbol{MH_t} - \boldsymbol{\mu_0}) \tag{3.3}$$

The MHWMA control chart signals an OOC when $T_t^2 > h$ and h is the chart design parameter chosen alongside w to achieve the desired in-control performance.

4 The Design Structure of the Proposed MDHWMA Control Chart

Like already highlighted, the EWMA chart and all control charts based on the EWMA structure assign larger weights to the most current observation and lesser weights to the less current observations. But Hunter (1986) showed that the main drawback of the plotting statistic of the EWMA chart lies in this manner of assignment of weights. And as a way of solution to this, Abbas (2018) designed and studied the homogeneously weighted moving average (HWMA) charting scheme which assigns a certain weight to the current process observation and the remaining weight is homogeneously assigned to the rest of the observations of the process. The chart showed a stronger detection strength compared to the EWMA chart for smaller OOC shifts. Abid et al. (2020) extended HWMA control chart to DHWMA control chart which increased the sensitivity of the former. In line with this augment, we are motivated to extend the work (MHWMA control chart) by Adegoke et al. (2019) to the Double MHWMA which will be written as MDHWMA control chart from hence forth with the intention of increasing the sensitivity of MHWMA control chart. This is because, in addition to assigning a specific weight to the current observation and the remaining weights being equally assigned to the previous $t-1$ observations, MDHWMA control chart utilizes the information from the process twice. Following the multivariate random variable setting already defined in Section 3, the charting statistic of the MDHWMA control chart is as in equation (4.1), where H_t is as defined in equation (3.2) of Section 3.

$$MD\boldsymbol{H_t} = w\boldsymbol{H_t} + (1-w)\,\bar{\bar{\boldsymbol{Y}}}_{\boldsymbol{t-1}} \tag{4.1}$$

where MH_t is as was given in equation (3.1). By substituting equation (3.2) in (4.1) and evaluating, we have

$$\begin{aligned}
\boldsymbol{MDH_t} &= w\left[w\bar{\boldsymbol{Y}}_{\boldsymbol{t}} + (1-w)\,\bar{\bar{\boldsymbol{Y}}}_{\boldsymbol{t-1}}\right] + (1-w)\,\bar{\bar{\boldsymbol{Y}}}_{\boldsymbol{t-1}} \\
&= w^2\bar{\boldsymbol{Y}}_{\boldsymbol{t}} + w\,(1-w)\,\bar{\bar{\boldsymbol{Y}}}_{\boldsymbol{t-1}} + (1-w)\,\bar{\bar{\boldsymbol{Y}}}_{\boldsymbol{t-1}} \\
&= w^2\bar{\boldsymbol{Y}}_{\boldsymbol{t}} + [w\,(1-w) + (1-w)]\,\bar{\bar{\boldsymbol{Y}}}_{\boldsymbol{t-1}} \\
&= w^2\bar{\boldsymbol{Y}}_{\boldsymbol{t}} + \left(1-w^2\right)\bar{\bar{\boldsymbol{Y}}}_{\boldsymbol{t-1}}
\end{aligned}$$

From Adegoke et al. (2019), the mean and covariance of $\boldsymbol{MDH_t}$ can be inferred to be $E(\boldsymbol{MDH_t}) = \mu_0$ and $\Sigma_{\boldsymbol{MDH_t}} = \frac{w^4}{n}\boldsymbol{\Sigma_0}$ for $t = 1$ and $\Sigma_{\boldsymbol{MDH_t}} = \frac{w^4}{n}\Sigma_0 + \left(1-w^2\right)^2 \frac{\Sigma_0}{n(t-1)}$ for $t > 1$, see the appendix for the details of the proof. Note that in the

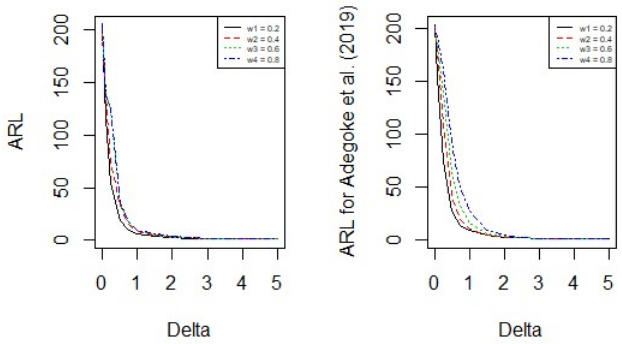

Figure 1: ARL respective plots of the MDHWMA control chart and the MHWMA control for $p = 2$, w =0.2, 0.4, 0.6 and 0.8 and for all shift sizes

case where $n = 1$, equation (14) simplifies to $\boldsymbol{MDH_t} = w^2\boldsymbol{Y_t} + \left(1 - w^2\right)\bar{\boldsymbol{Y}}_{\boldsymbol{t-1}}$, $\Sigma_{\boldsymbol{MDH_t}}$ simplifies to $w^4\Sigma_0$ for $t = 1$ and $w^4\Sigma_0 + \left(1 - w^2\right)^2 \frac{\Sigma_0}{(t-1)}$ for $t > 1$. The MDHWMA control chart statistic is given by

$$T_t^2 = \left(\boldsymbol{MDH_t} - \boldsymbol{\mu_0}\right)' \Sigma_{\boldsymbol{MDH_t}}^{-1} \left(\boldsymbol{MDH_t} - \boldsymbol{\mu_0}\right) \tag{4.2}$$

The MDHWMA control chart signals an OOC when $T_t^2 > h$ and h is the chart design parameter chosen alongside w to achieve the desired in-control performance. The method to obtain the different values of h will be discussed in Section 5 (Simulation Study).

5 Simulation Study

In this section, we access the performance of the MDHWMA control chart in terms of the run-length (RL) distribution and its characteristics. Specifically, we consider the ARL, MRL, and SDRL properties of the RL distribution. A chart with the smallest ARL_1 when compared to other similar charts performing under the same condition is said to have a better performance. Through simulation, the ARL, SDRL, and the MRL run length properties of the proposed chart would be generated to evaluate the performance and hence, compare it with the existing ones. The SDRL measures the spread of the run-length distribution of the ARL and the smaller the values of the OOC SDRL ($SDRL_1$) compared with those from other competing charts, the better the performance of the former (Human et al., 2011). The result of the evaluation is based on 10^5 Monte Carlo simulations run in the R programming language. To study the performance of the proposed chart and compare it with the existing memory-type control charts, we considered various combinations of the design parameters p, w and UCL needed to deliver the desired ARL_0. At each point in time, P and w are fixed while the value of the UCL needed to give the ARL_0 of 200 is carefully searched for. Table 3 contains the UCL values for each combination of P and w where P = 2, 3, 4, 5, 10 and w = 0.2, 0.4, 0.6, 0.8. It is important to note that for each value of P,

Table 1: The simulated data according to (Crosier, 1988)

	Observations		MDHWMA vector		
t	Y_1	Y_2	MDH_{t1}	MDH_{t2}	T_t^2
1	-1.19	0.59	-0.0476	0.0236	3.2884
2	0.12	0.9	-1.1376	0.6024	3.3829
3	-1.69	0.4	-0.5812	0.7312	3.7411
4	0.3	0.46	-0.8712	0.6232	7.2984
5	0.89	-0.75	-0.5548	0.5340	5.1105
6	0.82	0.98	-0.2686	0.3464	2.0454
7	-0.3	2.28	-0.1320	0.5040	2.9035
8	0.63	1.75	-0.1188	0.7364	6.4440
9	1.56	1.58	0.0120	0.8564	**8.2567**
10	1.46	3.05	0.1800	0.9956	**10.8258**

the multivariate normal distribution considered for simulation is the one with a mean vector of zero entries and variance-covariance matrix of unity leading diagonal and zero off-diagonal entries.

By making use of the values in Table 3, Table 4, Table 5, Table 6, Table 7 and Table 8, which contain the $ARLs$ of the proposed chart for the various values of P and w and for δ = 0.0, 0.1, 0.5, 0.75, 1.0, 1.5, 2, 0, 2.5, 3.0, 5.0 were obtained. Note that δ is the size of shift from the IC mean vector of the multivariate normal distribution, that is, for instance, for a shift of 0.1, the mean of each variable in the vector of variables is shifted by 0.1 and so on and so forth. In line with what exists in the literature (Adegoke et al., 2019), the OOC detection strength of the proposed chart deteriorates with increasing values of w. This is because both the values of the ARL_1 and MRL_1 are seen to be increasing with increasing values of w which implies a longer delay in an OOC signal. Though this characteristic is observed in Table 4, Table 5, Table 6 Table 7 and Table 8, but Table 4 will be used for discussion. Going by Table 4 and considering the two bold-faced lines which stand for the ARL and MRL of the proposed chart, one discovers that at $\delta = 0.25$ for instance, ARL_1 = **54.60, 74.02, 124.01, 125.04**, and MRL_1 = **36.5, 65.00, 99.5, 100.4** for w = **0.2, 0.4, 0.6** and **0.8** respectively and this clearly shows an increasing trend of the ARL_1 and MRL_1 with increasing value of w. Therefore, among all the values of w considered, the optimal value is 0.2 since the value combined with other parameters gave the longest IC ARL and the shortest $ARL_1$when compared with other values of w.

In an attempt to compare the sensitivity of the proposed chart with that of Adegoke et al. (2019), Table 1 of the Adegoke et al. (2019) is reproduced here as Table 9. Considering Table 4 of this work which is for $P = 2$ and comparing it at δ=0.25, w = 0.2, 0.4, 0.6, and 0.8 with Table 1 Adegoke et al. (2019) under the same condition, one discovers a much longer delay in an OOC signals of **74.00, 107.64, 139.03** and **161.6** by the MHWMA control chart which are contradicted with quicker OCC signals of **54.60, 74.02, 124.01** and **125.04** by the MDHWMA control chart of this work. Note that

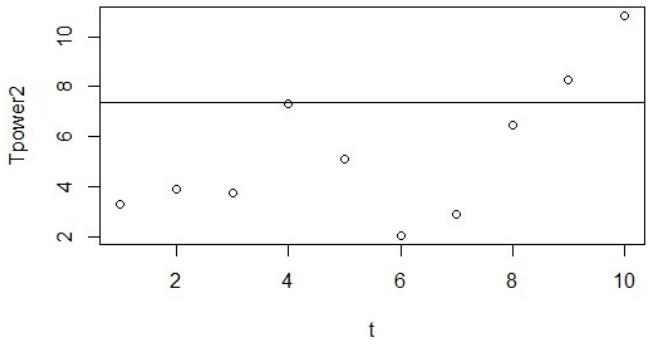

Figure 2: Plot of the MDHWMA control chart (T^2 as presented in Table 1) against the sample number (t)

Table 2: A Table lifted from Adegoke et al. (2019) for the MHWMA control chart to assist comparison in this work

	Observations		MHWMA vector		
t	Y_1	Y_2	H_{t1}	H_{t2}	T_t^2
1	-1.19	0.59	-0.0476	0.0236	3.29
2	0.12	0.9	-1.1376	0.6024	3.52
3	-1.69	0.4	-0.5812	0.7312	4.47
4	0.3	0.46	-0.8712	0.6232	7.15
5	0.89	-0.75	-0.5548	0.5340	3.97
6	0.82	0.98	-0.2686	0.3464	2.07
7	-0.3	2.28	-0.1320	0.5040	4.47
8	0.63	1.75	-0.1188	0.7364	7.45
9	1.56	1.58	0.0120	0.8564	8.71
10	1.46	3.05	0.1800	0.9956	**13.85**

Table 3: Control limit coefficient of the proposed MDHWMA chart

		Sensitivity Parameter (w)			
		0.2	0.4	0.6	0.8
Vector of the	2	7.35	9.87	10.525	10.525
number of variable (P)	3	7.5	11.7	12.5	12.7
	4	9.2	13.02	14.085	14.50
	5	12.23	16.0	16.8	16.801
	10	18.73	24.89	25.20	25.36

similar observations are seen with other shift sizes. This comparison was equally done graphically but for all shift sizes (delta) and for the same $P = 2$ and $w = 0.2$, 0.4, 0.6, and 0.8. The graphs for the two control charts (MHWMA control chart and MDHWMA control chart) were placed side-by-side in Figure 1. Looking at the graphs, it can be

Table 4: The ARL, SDRL AND MRL of the MDHWMA chart for $P = 2$

		Levels of Shift (δ)										
w		0.00	0.10	0.25	0.50	0.75	1.00	1.50	2.00	2.50	3.00	5.00
	ARL	**204.52**	**116.74**	**54.60**	**18.76**	**9.00**	**6.60**	**3.86**	**2.76**	**1.62**	**1.42**	**1.00**
w=0.2	SDRL	177.25	104.22	51.84	17.04	7.40	3.78	2.07	1.61	0.95	0.84	0.00
	MRL	**118.5**	**86.5**	**36.5**	**7.0**	**7.00**	**6.0**	**3.50**	**3.00**	**1.00**	**1.00**	**1.00**
	ARL	**196.82**	**138.40**	**74.02**	**33.96**	**15.40**	**8.86**	**5.26**	**3.26**	**2.24**	**1.72**	**1.00**
w=0.4	SDRL	166.52	89.46	50.64	19.48	8.04	5.76	2.55	1.37	1.08	0.90	0.00
	MRL	**158.0**	**119.5**	**65.00**	**29.00**	**15.5**	**8.0**	**5.00**	**3.00**	**2.00**	**1.00**	**1.00**
	ARL	**205.76**	**138.84**	**124.01**	**35.22**	**16.32**	**9.48**	**5.20**	**3.12**	**2.18**	**1.88**	**1.02**
w=0.6	SDRL	173.54	114.24	87.41	30.89	12.25	6.86	3.22	1.48	1.30	0.72	0.14
	MRL	**150.0**	**110.0**	**99.50**	**23.0**	**10.50**	**7.00**	**4.00**	**3.00**	**2.00**	**2.00**	**1.00**
	ARL	**205.79**	**138.89**	**125.04**	**36.202**	**17.36**	**9.88**	**6.201**	**3.77**	**2.19**	**1.98**	**1.06**
w=0.8	SDRL	173.59	114.35	87.45	30.99	12.35	6.77	3.21	1.57	1.31	0.73	0.15
	MRL	**151.0**	**111.0**	**100.40**	**24.0**	**11.10**	**7.50**	**4.20**	**3.10**	**2.09**	**2.10**	**1.00**

Table 5: The ARL, SDRL AND MRL of the MDHWMA chart for $P = 3$

		Levels of Shift (δ)										
w		0.00	0.10	0.25	0.5	0.75	1.0	1.5	2.0	2.5	3.0	5.0
	ARL	**192.32**	**119.74**	**49.54**	**18.54**	**9.40**	**6.54**	**3.28**	**3.02**	**2.02**	**1.62**	**1.04**
w= 0.2	SDRL	205.61	130.25	46.81	16.09	6.58	4.75	2.12	1.35	1.22	1.03	0.28
	MRL	**107.0**	**72.0**	**36.0**	**14.0**	**8.0**	**5.0**	**3.5**	**3.0**	**1.00**	**1.00**	**1.00**
	ARL	**198.28**	**152.28**	**65.98**	**28.52**	**16.50**	**8.70**	**5.56**	**3.04**	**2.46**	**1.80**	**1.06**
w= 0.4	SDRL	157.71	133.23	49.25	18.21	8.86	4.89	2.46	1.54	1.03	1.12	0.31
	MRL	**137.50**	**120.5**	**64.0**	**28.0**	**14.0**	**8.00**	**5.0**	**3.00**	**3.0**	**1.0**	**1.0**
	ARL	**202.02**	**172.30**	**108.04**	**40.88**	**18.76**	**11.76**	**5.44**	**3.54**	**2.44**	**1.68**	**1.08**
w= 0.6	SDRL	176.03	122.68	77.87	31.00	16.83	7.33	2.76	2.13	0.99	0.82	0.27
	MRL	**130.0**	**164.0**	**80.5**	**36.00**	**14.0**	**9.50**	**5.0**	**3.0**	**3.0**	**2.0**	**1.00**
	ARL	**205.64**	**195.52**	**124.06**	**82.60**	**36.26**	**25.22**	**9.20**	**3.42**	**2.60**	**1.92**	**1.06**
w= 0.8	SDRL	182.02	174.15	111.28	64.23	30.88	23.03	8.04	2.62	1.14	1.03	0.24
	MRL	**134.0**	**130.01**	**86.0**	**73.50**	**25.0**	**16.50**	**7.50**	**3.0**	**3.0**	**2.0**	**1.0**

seen that for all the values of w and for small to moderate shift sizes (say $\delta < 2.0$), the MDHWMA control chart returned smaller OOC ARL when compared to the MHWMA control chart. Therefore, the proposed MDHWMA control chart outperformed the MHWMA control chart by (Adegoke et al., 2019). Also, in terms of the $SDRL_1$, it is noticed that the proposed MDHWMA control chart has smaller $SDRL_1$ values than the MHWMA control chart. For instance, considering the same Table 1 of Adegoke et al. (2019) and the Table of this work and for δ=0.25, the $SDRL_1$ are **60.41, 102.17, 137.16, 160.77** which show larger variations of the ARL_1 for the MHWMA control chart when compared with **51.84, 50.64, 87.41, 87.45** of the proposed MDHWMA control chart of this work.

Adegoke et al. (2019) compared the ARL performance of the MHWMA control chart with that of the χ^2-control chart by Hotelling (1947), the MCUSUM control chart by Crosier (1988), the MCI control chart by Pignatiello and Runger (1990) and with that of the MEWMA control chart by Lowry et al. (1992). It was discovered and reported in Adegoke et al. (2019) that the Hotelling's chart, the MCUSUM chart, the MCI,

Table 6: The ARL, SDRL AND MRL of the MDHWMA chart for $P = 4$

		Levels of Shift (δ)										
w		0.0	0.1	0.25	0.5	0.75	1.0	1.5	2.0	2.5	3.0	5.0
	ARL	203.56	107.64	55.34	17.36	7.94	6.60	3.66	2.98	2.08	1.68	1.02
w= 0.2	SDRL	212.76	115.85	44.62	18.40	7.54	5.17	2.12	1.62	1.31	0.94	0.14
	MRL	151.5	66.0	52.0	12.0	6.0	5.0	3.0	3.0	1.0	1.0	1.0
	ARL	208.22	109.30	64.60	30.52	13.58	7.64	5.30	3.04	2.62	1.80	1.04
w= 0.4	SDRL	101.80	92.93	44.79	20.43	9.13	5.29	2.89	1.38	1.29	0.98	0.20
	MRL	171.0	73.5	66.0	25.5	11.0	6.5	5.0	3.0	3.0	1.5	1.0
	ARL	201.78	142.52	80.82	30.34	12.38	13.0	4.64	3.54	2.46	2.08	1.08
w= 0.6	SDRL	165.68	189.43	66.50	24.81	8.51	8.77	2.54	1.61	1.11	0.80	0.27
	MRL	164.5	88.5	64.5	21.5	10.0	12.0	4.0	3.0	2.0	2.0	1.0
	ARL	201.78	141.84	113.16	77.94	34.80	20.68	10.88	3.94	2.80	2.08	1.08
w= 0.8	SDRL	167.11	180.10	107.48	84.42	31.20	17.73	9.94	2.53	1.71	1.18	0.27
	MRL	149.11	87.0	71.0	54.5	31.0	15.0	7.0	3.5	2.0	2.0	1.0

Table 7: The ARL, SDRL AND MRL of the MDHWMA chart for $P = 5$

		Levels of Shift (δ)										
w		0.0	0.1	0.25	0.5	0.75	1.0	1.5	2.0	2.5	3.0	5.0
	ARL	204.32	160.26	73.12	31.50	12.90	9.10	5.56	3.50	2.28	1.90	1.0
w= 0.2	SDRL	222.84	153.83	56.24	22.87	8.87	6.56	3.15	1.26	1.26	1.15	0.0
	MRL	137.0	115.5	69.0	30.0	11.5	8.0	5.0	1.0	3.0	1.0	1.0
	ARL	204.32	134.86	77.02	36.28	20.34	11.14	5.72	4.0	3.0	2.22	1.08
w= 0.4	SDRL	185.95	104.13	59.10	22.90	11.69	6.67	2.99	1.74	1.23	1.06	0.34
	MRL	126.5	107.0	67.0	29.0	17.0	9.0	5.5	4.0	3.0	2.5	1.0
	ARL	198.66	187.04	126.20	58.50	25.24	16.50	5.82	3.70	2.52	2.02	1.10
w= 0.6	SDRL	207.78	167.01	98.53	55.56	19.40	12.97	3.96	1.73	1.09	0.84	0.30
	MRL	138.5	133.0	93.5	41.0	19.5	13.5	5.0	3.0	3.0	2.0	1.0
	ARL	205.80	191.14	137.94	104.0	64.68	36.96	9.74	5.28	2.90	2.0	1.04
w= 0.8	SDRL	212.15	199.09	117.31	87.41	55.07	28.82	8.19	3.59	1.69	1.16	0.20
	MRL	177.5	133.0	100.5	80.0	42.0	27.5	6.5	4.5	2.0	2.0	1.0

and the MEWMA charts based on the asymptotic covariance structure are inferior to the MHWMA control chart as the latter has the smallest ARL_1 across all shift sizes. Adegoke et al. (2019) equally discovered and noted in the paper that MHWMA control chart based on the exact covariance structure, detects shifts more than the MEWMA control chart when $\delta \leq 0.5$. Therefore, the findings of Adegoke et al. (2019) showed that the MHWMA control chart outperformed the competing memory-type charts in detecting small shifts from the IC targets. However, in this paper, it has been shown that the MDHWMA control chart is superior to the MHWMA control chart in OCC detection strength. Therefore, it implies that the MDHWMA control chart outsmarted the existing competing memory-type charts.

6 Numerical Application of the MDHWMA-chart

In this section, the application of the MDHWMA control chart is provided based on simulated data-set following (Crosier, 1988). The data consists of 10 observations with the first five being IC state with the mean vector, μ_0= (0, 0) and the remaining five are OOC at $\boldsymbol{\mu_1}$= (1, 2). The same data-set has been used to illustrate the application of multivariate control charts, see Lowry et al. (1992) and Adegoke et al. (2019). In this illustration, the data is a bivariate data, therefore, $P = 2$ and a sensitivity parameter of ($w = 0.2$) will be used. Given these specifications, $h = 7.35$ desired to achieve the ARL_0 of 200. Note that the value of h is obtained through simulation for particular values of w and ARL desired in the monitoring process. That is, by using a simulation study to search for the value of h for which the MDHWMA control chart delivers the desired IC $ARL = 200$ as considered in this work and in Adegoke et al. (2019) for some fixed values of P and w. The values of h obtained for the various values of P and w are presented in Table 3. With the above provisions and definitions, apply the MDHWMA control chart as follows;

1. Use the final evaluation of equation (14) to calculate the value of MDH_t from the data for each t = 1, 2, 3, ..., 10.

2. Obtain the value of $\Sigma^{-1}_{MDH_t}$ from the Σ_{MDH_t} and hence, obtain the values of T_t^2 for each t using equation (4.2).

The real data, the calculated values of MDH_t and T_t^2 from steps 1 and 2 are presented in Table 1 Recall that $T_t^2 > h$ declares a sample OOC and IC if otherwise. From Table 1, it is seen that samples (9) and (10) with T^2-values of **8.2567** and **10.8258** are all greater that $h =$ **7.35**, therefore, the samples have been declared OOC by the MDHWMA control chart. For a clearer picture of this OOC declaration by the chart, the graph of the control statistics $\left(T_t^2\right)$ against the sample number (t) has been included in Figure 2 and looking at it equally, two sample point (samples 9 & 10) fell out of the control region and were as such declared OOC.

However, according to the MHWMA control chart of Adegoke et al. (2019), only the 10^{th} sample was declared OOC with a T^2-value of 13.85 at $w = 0.10$ as reproduced in Table 2 of this work. Also, when $w = 0.20$ is applied in the design of the MHWMA control chart, the T^2-values of the samples from the first to the last are; 3.2884, 3.7085, 5.7835, 6.3952, 2.0098, 1.9946, 7.2145, 8.2607, 8.4849 and **17.0241** respectively. Note that according to Table 1 of Adegoke et al. (2019) reproduced in Table 9 in this work, when $P = 2$ and $w = 0.20$, h is **10.19**. Therefore, comparing the values of the T^2 for the samples with $h =$**10.19**, it is seen that only the 10^{th} sample is still declared OOC by the MHWMA control chart. However, MDHWMA control chart at the same conditions declared the 9^{th} and the 10^{th} samples OOC as can be seen in Table 1 of this work and by implication also, the MDHWMA control chart has edge over the MHWMA-chart in an OOC detention strength and hence a better chart over the MHWMA control chart.

Table 8: The ARL, SDRL AND MRL of the MDHWMA chart for $P = 10$

		Levels of Shift (δ)										
w		0.0	0.1	0.25	0.5	0.75	1.0	1.5	2.0	2.5	3.0	5.0
	ARL	**203.20**	**172.84**	**64.94**	**26.88**	**17.10**	**9.70**	**5.44**	**3.86**	**3.08**	**2.04**	**1.08**
w= 0.2	SDRL	210.0	154.25	70.41	22.42	12.23	6.13	2.97	2.03	1.58	1.19	0.40
	MRL	128.5	137.7	42.5	22.5	15.5	9.0	5.0	4.0	3.0	1.0	1.0
	ARL	**200.58**	**174.26**	**115.62**	**43.60**	**23.28**	**12.60**	**7.16**	**4.84**	**3.44**	**2.48**	**1.18**
w= 0.4	SDRL	160.15	180.33	90.86	27.40	13.43	6.65	2.53	2.44	1.18	1.13	0.44
	MRL	159.5	155.0	86.5	37.0	22.5	12.0	6.5	5.0	4.0	3.0	1.0
	ARL	201.92	175.28	157.38	86.50	31.76	16.94	9.12	4.88	3.28	2.30	1.16
w= 0.6	SDRL	197.05	197.09	146.84	73.72	25.86	11.48	6.12	2.47	1.44	0.89	0.37
	MRL	137.0	95.0	109.5	58.0	23.5	16.0	7.5	5.0	3.0	2.0	1.0
	ARL	200.09	178.28	159.38	88.50	35.76	20.94	10.12	5.88	4.28	2.50	1.26
w= 0.8	SDRL	198.05	199.09	147.84	75.72	27.86	12.48	6.15	2.49	1.51	0.99	0.38
	MRL	138.0	99.0	119.5	62.0	26.5	18.0	8.0	5.5	3.7	2.21	1.0

Table 9: ARL-values of MHWMA-chart for $(P = 2)$

	w=0.03		w=0.05		w=0.2		w=0.4		w=0.6		w=0.8	
δ	ARL	SDRL	ARL	SDRL	ARL	SDRL	ARL	SDRL	ARL	SDRL	ARL	SDRL
0	199.26	202.35	199.35	182.57	202.99	186.06	201.63	192.36	200.54	201.62	200.39	199.06
0.05	166.24	197.29	173.00	157.48	186.94	169.67	193.77	189.26	194.31	190.36	199.62	198.50
0.10	115.64	132.81	129.55	119.99	154.16	136.29	177.88	173.09	184.99	185.98	192.07	194.5
0.25	43.03	44.91	53.32	46.28	74.00	60.41	107.64	102.17	139.03	137.16	161.6	160.77
0.50	15.80	14.3	19.87	15.56	27.50	19.50	41.84	36.40	64.86	62.32	91.91	90.24
0.75	8.56	6.83	10.65	7.7	14.50	9.24	19.25	15.5	31.66	29.95	50.15	49.11
1.00	5.70	4.09	6.91	4.52	9.23	5.31	10.94	7.96	16.54	14.56	27.24	26.23
1.50	3.32	2.04	3.90	2.22	4.85	2.48	5.05	3.05	6.3	4.8	9.67	8.71
2.00	2.32	1.4	2.67	1.49	3.19	1.49	3.13	1.62	3.41	2.2	4.54	3.63
2.50	1.74	1.06	1.99	1.16	2.35	1.12	2.22	1.05	2.26	1.2	2.66	1.79
3.00	1.37	0.79	1.53	0.9	1.81	0.90	1.70	0.76	1.7	0.79	1.86	1.07
5.00	1.00	0.08	1.01	0.09	1.03	0.17	1.03	0.16	1.03	0.18	1.03	0.17
h	5.40		6.79		10.19		10.56		10.61		10.62	

7 Conclusion

In this work, a MDHWMA control chart was proposed and the performance in terms of the run length properties evaluated using Monte Carlo simulation. The comparison of the MDHWMA control chart with the MHWMA control chart and in relation with some other competing charts was considered. The comparison showed that the MDHWMA control chart outsmarted the MHWMA control chart which implies that it equally did to the other competing charts in OOC detection, especially at small to moderate sizes of δ since it has been established in the lietrature that MHWMA control chart is better than the other competing charts in OOC detection.

It was equally discovered that the OOC detection strength of the proposed MDHWMA control chart is inversely proportional to the size of w, the sensitivity parameter. Furthermore, when P, which stands for the number of variables in the vector of variables was varied, it was not seen to affect the performance of the MDHWMA control chart significantly in detecting the OOC situations. It would be nice if this work, as a way

of further research, is extended to a multivariate triple homogeneous weighted moving average control chart, that is, MTHWMA control chart. Again, it might be a novelty considering some modifications in these multivariate quality control charts designs to allow their application to non-normal multivariate data/observations.

References

Abbas N. Homogeneously weighted moving average control chart with an application in substrate manufacturing process. Computers and Industrial Engineering. 2018;120(2):460–470. https://doi.org/10.1016/j.cie.2018.05.027.

Abbas N, Riaz M, Does RJMM. Mixed exponentially weighted moving average-cumulative sum charts for process monitoring. Quality and Reliability Engineering International. 2013;29(3):345–356. https://doi.org/10.1002/qre.1391.

Abbas Z, Nazir HZ, Akhtar N, Riaz M, Abid M. On developing an exponentially weighted moving average chart under progressive setup: An efficient approach to manufacturing processes. Quality and Reliability Engineering International. 2020;36(8):2569–2591. https://doi.org/10.1002/qre.2660.

Abbasi SA, Riaz M, Miller A, Ahmad S, Nazir HZ. EWMA dispersion control charts for normal and non-normal processes. Quality and Reliability Engineering International. 2015;31(8):1691–1704. https://doi.org/10.1002/qre.1660.

Abid M, Shabbir A, Nazir HZ, Sherwani RAK, Riaz M. A double homogeneously weighted moving average control chart for monitoring of the process mean. Quality and Reliability Engineering International. 2020;36(1):1513–1527. https://doi.org/10.1002/qre.2591.

Adegoke NA, Abbasi SA, Smith ANH, Anderson MJ, Pawley MDM. A multivariate homogeneously weighted moving average control chart. IEEE Access. 2019;7(1):9586–9597. https://doi.org/10.1109/ACCESS.2019.2890780.

Aslam M, Bhattacharya R, Aldosari MS. Design of control chart in presence of hybrid censoring scheme. IEEE Access. 2018;6(1):14895–14907. https://doi.org/10.1109/ACCESS.2018.2817583.

Crosier RB. Multivariate generalizations of cumulative sum quality-control schemes. Technometrics. 1988;30(3):291–303. https://doi.org/10.1080/00401706.1988.10488407.

Hawkins DM, Maboudou-Tchao EM. Self-starting multivariate exponentially weighted moving average control charting. Technometrics. 2007;49(2):199–209. https://doi.org/10.1198/004017007000000125.

Hotelling H. Multivariate quality control illustrated by the air testing of sample bombsights. In: Eisenhart MWHC, Wallis WA, editors. Techniques of Statistical Analysis. New York, NY, USA: McGraw-Hill; 1947. p. 111–184.

Human SW, Kritzinger P, Chakraborti S. Robustness of the EWMA control chart for individual observations. Journal of Applied Statistics. 2011;38(10):2071–2087. https://doi.org/10.1080/02664763.2010.545117.

Hunter JS. The exponentially weighted moving average. Journal of Quality Technology. 1986;18(4):203–210.

Kramer HG, Schmid W. EWMA charts for multivariate time series. Sequential Analysis. 1997;16(2):131–154. https://doi.org/10.1080/07474949708836320.

Letshedi TI, Malela-Majika JC, Shongwe SC. New extended distribution-free homogeneously weighted monitoring schemes for monitoring abrupt shifts in the location parameter. PLOS ONE. 2022;17(1):e0262840. https://doi.org/10.1371/journal.pone.0262840.

Lowry CA, Woodall WH, Champ CW, Rigdon SE. A multivariate exponentially weighted moving average control chart. Technometrics. 1992;34(1):46–53. https://doi.org/10.1080/00401706.1992.10485232.

Lucas JM. Combined Shewhart-CUSUM quality control schemes. Journal of Quality Technology. 1982;14(2):51–59.

Lucas JM, Saccucci MS. Exponentially weighted moving average control schemes: Properties and enhancements. Technometrics. 1990;32(1):1–12. https://doi.org/10.1080/00401706.1990.10484583.

Luke P, Jean C, Malela-Majika JC, Schalk H, Philippe C. A new multivariate extended homogeneously weighted moving average monitoring scheme incorporated with a support vector machine. Quality and Reliability Engineering International. 2023;39(6):2454–2475. https://doi.org/10.1002/qre.3245.

Page ES. Continuous inspection schemes. Biometrika. 1954;41(1–2):100–115. https://doi.org/10.1093/biomet/41.1-2.100.

Park J, Jun CH. A new multivariate EWMA control chart via multiple testing. Journal of Process Control. 2015;26(1):51–55. https://doi.org/10.1016/j.jprocont.2014.10.003.

Pignatiello JJ, Runger GC. Comparisons of multivariate CUSUM charts. Journal of Quality Technology. 1990;22(3):173–186.

Roberts SW. Control chart tests based on geometric moving averages. Technometrics. 1959;1(3):239–250. https://doi.org/10.1080/00401706.1959.10489860.

Saber A, Zameer A, Hafiz ZN, Riaz M, Xingfa Z, Yuan L. On developing sensitive nonparametric mixed control charts with application to manufacturing industry. Quality and Reliability Engineering International. 2021;2021:1–25. https://doi.org/10.1002/qre.2898.

Seif A, Moghadam MB, Faraz A, Heuchenne C. Statistical merits and economic evaluation of T^2 control charts with the VSSC scheme. Arabian Journal for Science and Engineering. 2011;36(7):1461–1470. https://doi.org/10.1007/s13369-011-0139-z.

Shamma SE, Shamma AK. Development and evaluation of control charts using double exponentially weighted moving averages. International Journal of Quality and Reliability Management. 1992;9(6):18–25. https://doi.org/10.1108/02656719210019481.

Testik MC, Runger GC, Borror CM. Robustness properties of multivariate EWMA control charts. Quality and Reliability Engineering International. 2003;19(1):31–38. https://doi.org/10.1002/qre.525.

Yumin L. An improvement for MEWMA in multivariate process control. Computers and Industrial Engineering. 1996;31(3):779–781. https://doi.org/10.1016/0360-8352(96)00218-3.

Zaman B, Abbas N, Does RJMM. Mixed cumulative sum exponentially weighted moving average control charts. Quality and Reliability Engineering International. 2014;31(8):1407–1421. https://doi.org/10.1002/qre.1651.

APPENDIX: Derivation of the mean vector and covariance matrix of $\boldsymbol{MDH_t}$.

The $\boldsymbol{MDH_t}$ is given by $\boldsymbol{DMH_t} = w\boldsymbol{MH_t} + (1-w)\bar{Y}_{t-1}$, but $\boldsymbol{MH_t}$ is given by $w\boldsymbol{Y_t} + (1-w)\bar{\boldsymbol{Y}}_{\boldsymbol{t-1}}$, therefore, $\boldsymbol{MDH_t}$ is given by

$$w(w\boldsymbol{Y_t} + (1-w)\bar{\boldsymbol{Y}}_{\boldsymbol{t-1}}) + (1-w)\bar{\boldsymbol{Y}}_{\boldsymbol{t-1}}$$

$$= w^2\boldsymbol{Y_t} + w(1-w)\bar{\boldsymbol{Y}}_{\boldsymbol{t-1}} + (1-w)\bar{\boldsymbol{Y}}_{\boldsymbol{t-1}} \Rightarrow w^2\boldsymbol{Y_t} + [(w(1-w) + (1-w)]\bar{\boldsymbol{Y}}_{\boldsymbol{t-1}}$$

$$\therefore MDH_t = w^2\boldsymbol{Y_t} + (1-w^2)\bar{\boldsymbol{Y}}_{\boldsymbol{t-1}}$$

Therefore, we have that for an in-control situation, the mean vector of the $\boldsymbol{DMH_t}$ is given by

$$\begin{aligned} E\left(\boldsymbol{MDH_t}\right) &= E\left[w^2\bar{y}_t + \left(1-w^2\right)\bar{\bar{y}}_{t-1}\right] \\ &= w^2E\left(Y_t\right) + (1-w^2)E\left(\bar{Y}_{t-1}\right) \\ &= w^2\mu_0 + (1-w^2)\mu_0 = \boldsymbol{\mu_0} \end{aligned}$$

The covariance matrix. First, we consider when $t=1$ where $DMH_1 = w^2Y_1 + (1-w^2)\bar{Y}_0$ and $\bar{Y}_0 = \mu_0$, therefore, $DMH_1 = w^2Y_1 + (1-w^2)\mu_0$

$$\begin{aligned} Var\left(MDH_t\right) &= var\left(w^2Y_1\right) + var\left([1-w^2]\mu_0\right) \\ &= w^4\Sigma_0 \end{aligned}$$

For $t > 1$

$$Var\left(MDH_t\right) = var\left(w^2Y_t\right) + var\left([1-w^2]\bar{Y}_{t-1}\right) + 2w^2\left(1-w^2\right)cov\left(Y_1, \bar{Y}_{t-1}\right)$$

Recall that on the assumption that Y_t are independent and identically distributed, $Cov\left(Y_t, \bar{Y}_{t-1}\right) = 0$ and $Var\left(MDH_t\right)$ becomes;

$$w^2\Sigma_0 + \left(1-w^2\right)^2\frac{\Sigma_0}{t-1}.$$